

## Effect of built-up edge formation on residual stresses induced by dry cutting of normalized steel

Johannes Kümmel<sup>1,a,\*</sup>, Jens Gibmeier<sup>1,b</sup>, Volker Schulze<sup>1,2,c</sup>,  
Alexander Wanner<sup>1,d</sup>

<sup>1</sup>Karlsruhe Institute of Technology (KIT), Institute for Applied Materials (IAM), Kaiserstraße 12, D-76131 Karlsruhe, Germany

<sup>2</sup>Karlsruhe Institute of Technology (KIT), Institute for Production Science (wbk), Kaiserstraße 12, D-76131 Karlsruhe, Germany

<sup>a</sup>johannes.kuettel@kit.edu, <sup>b</sup>jens.gibmeier@kit.edu, <sup>c</sup>volker.schulze@kit.edu,  
<sup>d</sup>alexander.wanner@kit.edu

**Keywords:** machining, dry cutting, built-up edge, surface layer, cutting tool wear

**Abstract.** The tool and workpiece surface layer states of the tribosystem uncoated WC-Co cutting tools vs. normalised SAE 1045 workpiece material are studied in detail for a dry metal cutting process. Within the system the cutting parameters (cutting speed, feed rate, cutting depth) determine the wear state of the cutting tool and the resulting surface layer state (residual stress) in the workpiece. As the built-up edge can be used as a possible wear protecting layer [1] the influence of built-up edge and wear behaviour of the cutting tool was examined with respect to the workpiece surface layer state for knowledge based metal cutting processing. Small compressive stresses (-60 – -80 MPa) are induced in the surface layer, that are nearly homogeneous for the highest built-up edge, which lead to the lowest tool wear in combination with lowest cutting temperature.

### Introduction

At machining metals it is important to know about the wear behaviour of the cutting tool. This importance arises due to the fact, that the surface integrity of the machined workpiece is influenced by tool wear and built-up edge formation. In this case surface integrity is described by three main parameters: the surface roughness, the residual stress state and the work hardening in the surface zone [2,3,4]. In dry plain turning operation no coolant or lubricant is used to avoid any environmental influences by disposal. The high adhesion of the workpiece material to the cutting tool leads to a built-up edge formation, which can act as local cutting tool wear protecting layer [1]. The adhering built-up edge protects the flank face of the main cutting edge by flank wear due to the fact that the chip formation zone is displaced towards the “new” cutting edge of the adhering built-up edge. As a consequence the direct sliding movement between workpiece surface and flank face of the cutting tool is avoided [1]. For the application of a sufficiently stable built-up edge produced in the cutting process, the residual stress state has to be known to get a better process understanding of the dry metal cutting process. Some investigations with respect to residual stress depth profiles in machined workpieces induced by turning operation were carried out [2], whereas the main focus of interest was the surface integrity and residual stress state [5] in orthogonal (micro)cutting. Only few literature is available concerning the interaction of worn cutting tools on the residual stress state in the machined workpiece [6,7]. However, a detailed analysis of residual stress depth profiles in the regime of built-up edge formation in metal cutting processing has not been carried out yet.

Consequently, metal cutting was conducted with a cutting system, where built-up edge formation is provoked. SAE 1045 steel is used as workpiece material in a normalized state and uncoated cemented carbide cutting tools with a simple geometry and high cutting edge radius (30 µm) were used for the dry plain turning operation. By applying an entering angle of 45° the built-up edge could be conserved mostly on the cutting tool to check the dimensions of the built-up edge evolving on the rake face.

## Experimental Setup

Plain carbon steel type SAE 1045 in a normalized state was machined with an initial grain size of  $\approx 16 \mu\text{m}$  as workpiece material. Cylinders with lengths of 100 mm and with an initial diameter of 58 mm were produced as workpieces. Dry plain turning was applied using a machining centre Heller MC 16. The cutting tool (manufacturer: Walter AG) used for the experiments was industrial fine-grained cemented carbide (grade K10) with a composition of 94 vol.-% WC and 6 vol.-% Co in an uncoated state. This choice of cutting tool material promotes built-up edge formation due to adhesion tendency to the chosen workpiece material. The designation of the tool is SNMA 120408 according to the standard DIN ISO 1832 as a simple geometry. The cutting parameters are summarized in Fig. 1. A negative rake angle was chosen since it supports the built-up edge formation.

Cutting speed $v_c$ [m/min]	50 - 150
Feed rate $f$ [mm/rev]	0.05
Cutting depth $a_p$ [mm]	1.0
Rake angle $\gamma$ [°]	-8
Clearance angle $\alpha$ [°]	8
Wedge angle $\beta$ [°]	90
Corner radius $r_e$ [mm]	0.8
Entering angle $\kappa_r$ [°]	45
Initial cutting edge radius $r_\beta$ [ $\mu\text{m}$ ]	30

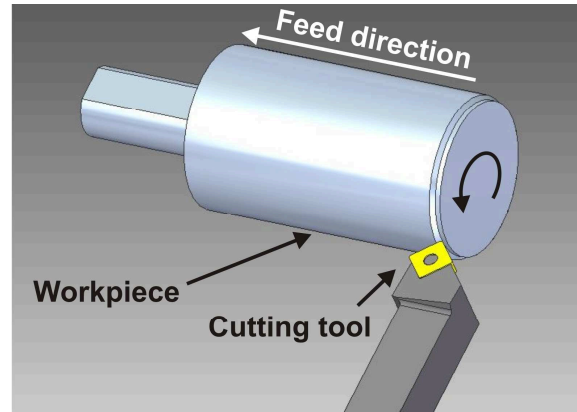


Fig. 1: Cutting parameters used in the experiments for provoked built-up edge formation and conservation of built-up edges on the cutting tool (see table on the left) and display of experimental setup for dry plain turning operation (see figure on the right).

Different wear tests were applied to reveal the influence of built-up edges on the wear state of the cutting tool. The parametric study of the machining was carried out by dry plain turning of the cylindrical workpieces (initial diameter = 58 mm) down to a diameter of 24 mm. The cutting tools were examined after different cutting lengths, where the built-up edge and the flank wear were documented by means of light optical microscopy. For the measurement of flank wear land width (VB), radius wear and built-up edge height the same method was applied as described in [1]. The average values of wear sizes were recorded after defined cutting lengths to reveal the wear evolution. As the aim of this research project is to check the influence of the built-up edge formation and cutting tool wear on workpiece surface layer state after different cutting lengths (corresponding to different wear states of the cutting tool) some sections of the workpiece material were cut and measured with respect to the residual stress state in the surface near regions (see Fig. 3). X-ray stress analysis was carried out for the near-surface regions according to the  $\sin^2\psi$ -method [8] to evaluate any changes in machining induced residual stresses, which are affected by built-up edge formation and cutting tool wear. The parameters used for residual stress analysis are summarized in Table 1.

Table 1: Parameters for X-ray residual stress analysis.

Radiation (k $\beta$ -filter)	Cr-K $\alpha$ (Vanadium)
Lattice planes	{211} of ferrite
X-ray elastic constant $s_1$ [MPa $^{-1}$ ]	$-1.27 \cdot 10^{-6}$ [9]
X-ray elastic constant $\frac{1}{2}s_2$ [MPa $^{-1}$ ]	$5.82 \cdot 10^{-6}$ [9]
Range in $\psi$ (13 tilt angles) - equidistant in $\sin^2\psi$ -	$-60^\circ < \psi < 60^\circ$

X-ray residual stress analysis was carried out using a diffractometer of type “Karlsruhe” used in  $\psi$ -mode. The primary X-ray beam was formed by a pinhole with a nominal diameter of 1 mm and a symmetrisation slit was used as secondary aperture [10]. The residual stress was measured on the surface and in the depth up to a surface depth of about 200  $\mu\text{m}$ . Disks of the turned workpiece material were sectioned and the residual stresses were measured in cutting direction (hoop component, see Fig. 3). The depth profile is acquired by successive electrochemical layer removal in combination with repeated X-ray stress analysis on the newly generated surface. The measured reflections of {211} ferrite lattice planes were fitted with Pearson VII functions. Slices from workpiece material were sectioned after four passes (corresponds to a cutting length  $l_c$  of 1332 m) and after 17 passes ( $l_c = 4030$  m).

## Results and Discussion

The cutting tools were examined after different cutting lengths in the cutting speed ( $v_c$ ) regime of 50 -150 m/min. The applied cutting speed has got quite different consequences on the cutting tool wear state and the built-up edge formation. For the measurement of flank wear land width VB and ex-situ determined built-up edge height the same procedure was used as previously published [1].

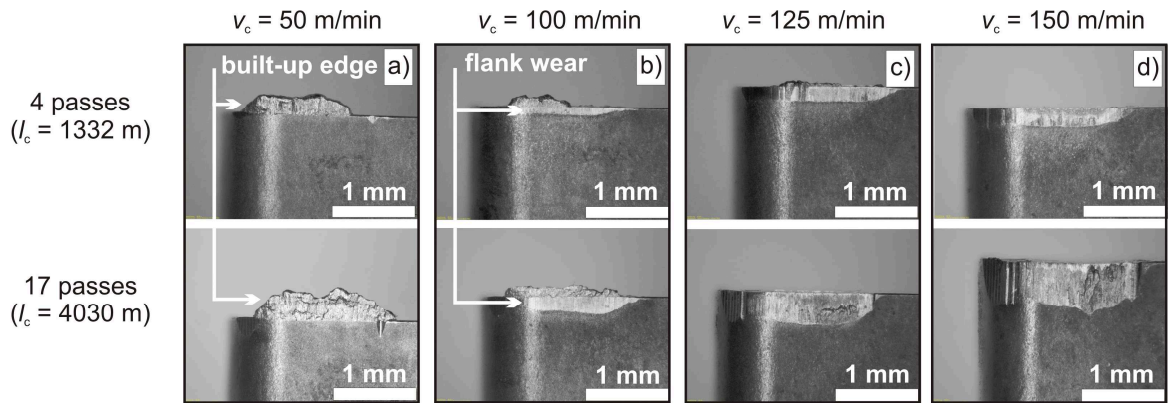


Fig. 2: Overview of flank faces (the adhering built-up edges and the flank wear are indicated) of cutting tools used in the dry metal cutting process. For the eight different tool wear states for four different cutting speeds  $v_c$  in the built-up edge formation regime (a):  $v_c = 50$  m/min; b):  $v_c = 100$  m/min; c):  $v_c = 125$  m/min; d):  $v_c = 150$  m/min) the resulting residual stress depth profiles for the corresponding machined workpieces are determined.

In Fig. 2 an overview of the eight different cutting tool states (with respect to built-up edge and wear state) are displayed for the corresponding residual stress depth profile analysis in the machined workpiece. A summary of flank wear land width VB values and built-up edge heights is shown in Table 2. The experimental procedure for the metal cutting process is shown in Fig. 3.

Table 2: Wear and built-up edge parameters for the different workpieces examined with respect to residual stress.

Cutting length $l_c$ [m]	Cutting speed [m/min]	Flank wear land width VB [ $\mu\text{m}$ ]	Built-up edge height [ $\mu\text{m}$ ]
1332 (corresponding to 4 passes)	50	0	$249 \pm 19$
	100	$86 \pm 13$	$129 \pm 14$
	125	$178 \pm 7$	$63 \pm 15$
	150	$222 \pm 13$	0
4030 (corresponding to 17 passes)	50	0	$360 \pm 48$
	100	$194 \pm 29$	$136 \pm 12$
	125	$371 \pm 27$	0
	150	$527 \pm 16$	0

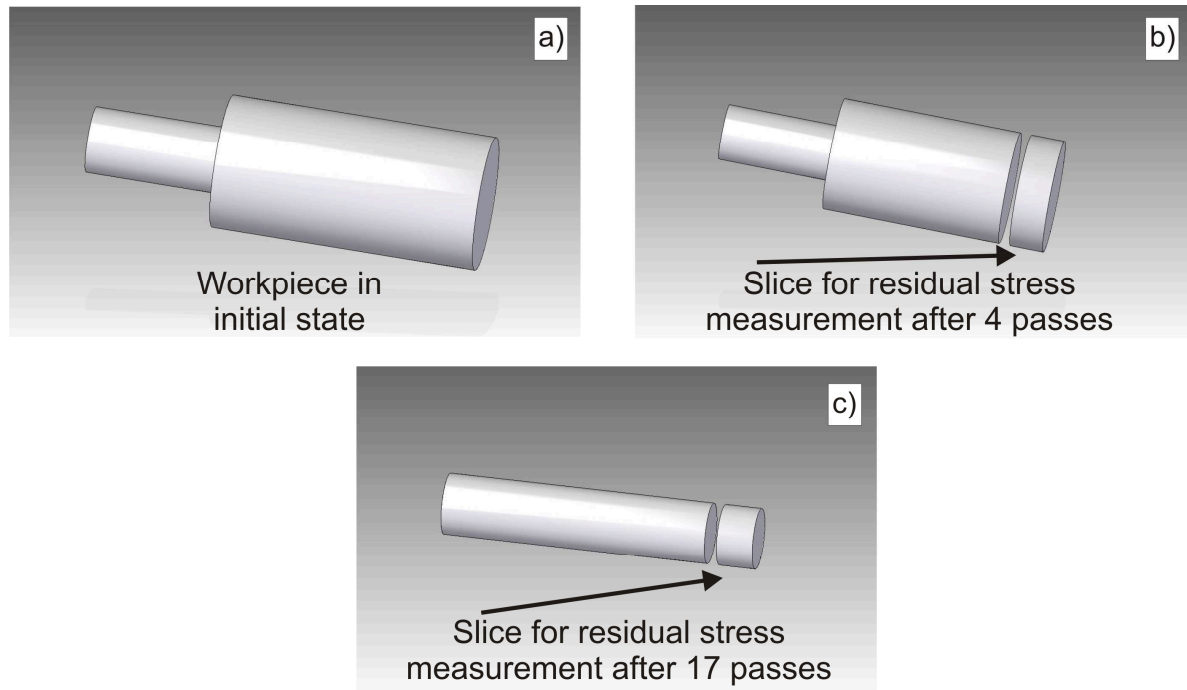


Fig. 3: Schematic overview of workpiece evolution from initial state a) (diameter of 58 mm) reducing to a diameter of 50 mm after four cutting passes b) to the final state after 17 passes c). The particular slices for residual stress measurement are marked with an arrow.

The residual stress depth profiles and depth profiles of the integral widths (IB) of the X-ray interference profiles for the cutting length of 1332 m (4 passes) are displayed in the following figure (Fig. 4).

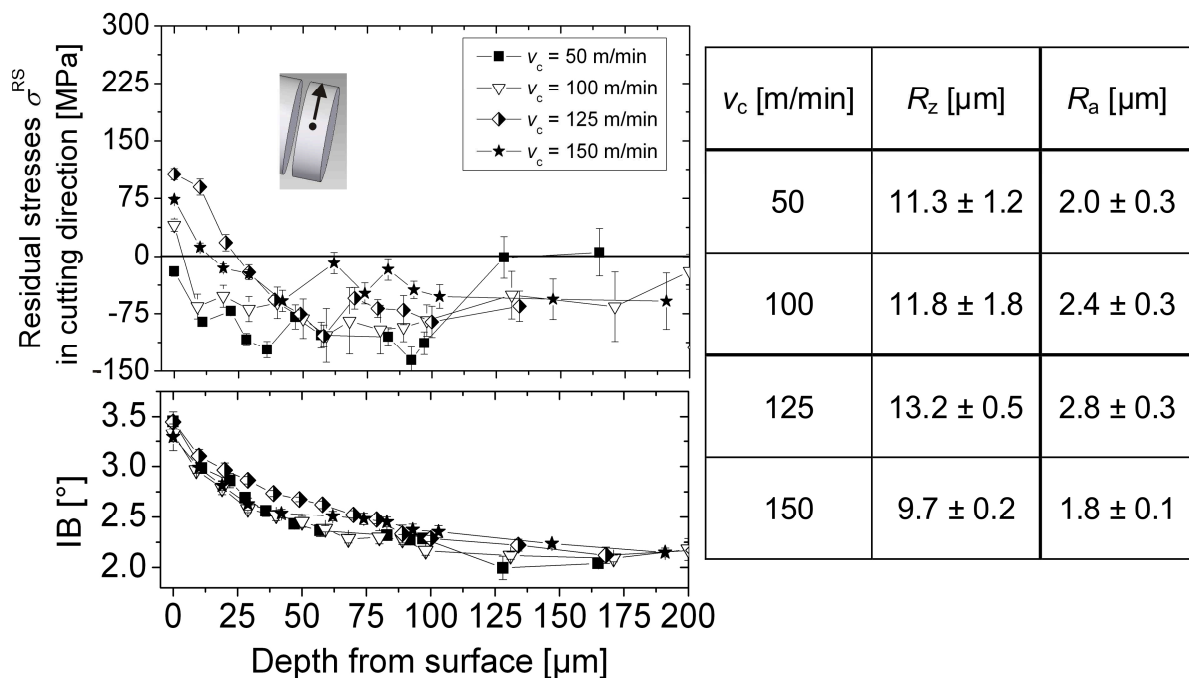


Fig. 4: Residual stress and IB depth profiles in workpiece surface layer for the different cutting speeds examined after 4 passes (resulting in different built-up edge heights and wear states of cutting tool) (see Table 2). The measurement point and measurement direction are indicated. Further, the surface roughness values ( $R_z$  and  $R_a$ ) of the machined workpiece (measured with confocal white light microscopy) are displayed in the table presented at the right hand side.

Fig. 4 shows an increasing tensile residual stress state at the very surface (increasing from about 40 MPa for the cutting speed of 100 m/min (built-up edge height = 129  $\mu\text{m}$ ) to a tensile stress of about 80 – 100 MPa for the highest cutting speeds applied (125 m/min and 150 m/min)). The lowest cutting speed with the most pronounced built-up edge leads to small compressive residual stresses ( $\approx -20$  MPa) in the surface with a nearly uniform compressive stress distribution of -87 MPa in a depth of about 20-80  $\mu\text{m}$ . The stress gradients for the higher cutting speeds (100 – 150 m/min) from surface to about 80  $\mu\text{m}$  into the workpiece are increasing with cutting speed. This seems to be mainly driven by higher cutting temperatures acting in the cutting zone by higher cutting speeds.

The integral width (IB) profiles shown in Fig. 4 indicate no significant influence of the applied cutting conditions (different cutting speeds) on the microstructural state. The highest value of about  $3.3^\circ$  is measured directly at the surface. This value is decreasing continuously to  $2.3^\circ$  for the unaffected workpiece interior for all cases studied. No significant difference in work hardening for the different cutting parameters, built-up edge heights and wear states of the cutting tools can be observed.

Residual stress analyses were carried out for workpieces, which were machined using worn tools (see Fig. 2 c) and d) for the cutting speeds of 125 m/min – 150 m/min) without built-up edges (see Table 2). Also a tool state without wear on the flank face (protected by high built-up edge height during the cutting process (see Fig. 2 a)) was considered ( $v_c = 50$  m/min) and a tool state with built-up edge and flank wear land width of 194  $\mu\text{m}$  ( $v_c = 100$  m/min) was applied for the determination of residual stress depth profiles in the resulting machined workpiece.

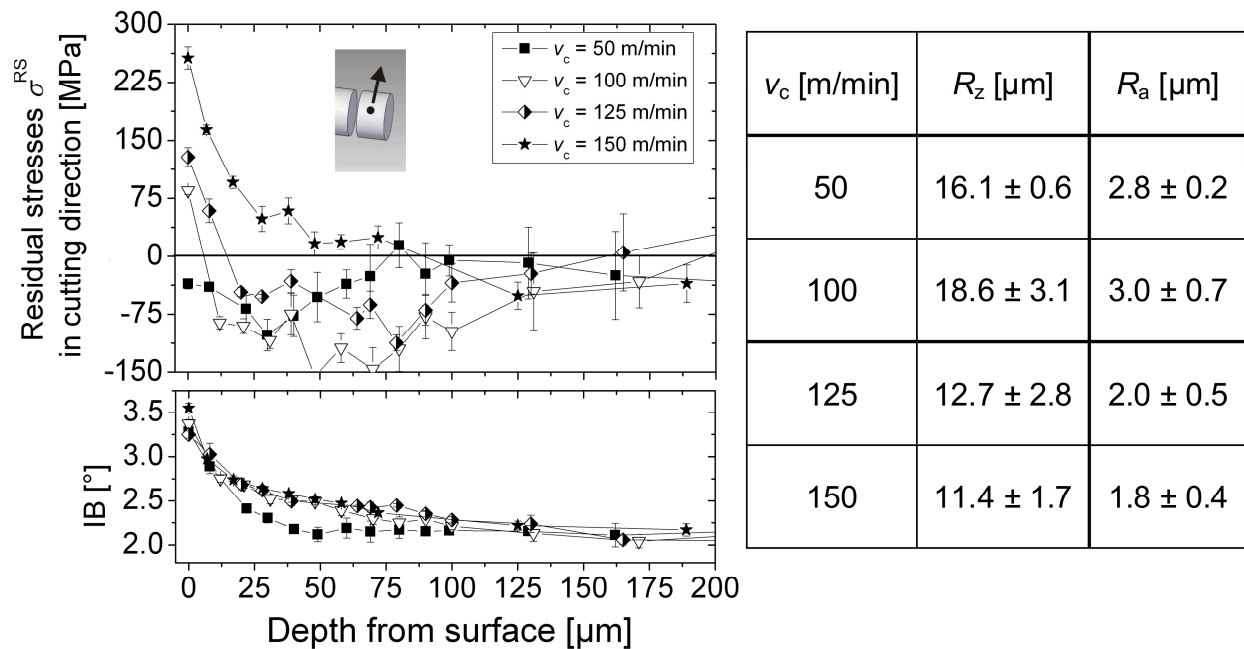


Fig. 5: Residual stress and IB depth profiles in workpiece surface layer for the cutting speeds used after 17 passes, which corresponds to  $l_c = 4030$  m (resulting in different built-up edge height and wear state of cutting tool) (see Table 2). The measurement point and measurement direction are indicated. Further, the surface roughness values ( $R_z$  and  $R_a$ ) of the machined workpiece (measured with confocal white light microscopy) are displayed in the table presented at the right hand side.

In Fig. 5 the residual stress depth profiles and integral width (IB) for the surface layer states in the workpiece for higher tool wear without built-up edge (for the cutting speeds of 125 m/min – 150 m/min) is shown. The used cutting tools had clearly higher tool wear (see Table 2, VB ( $v_c = 125$  m/min) = 371  $\mu\text{m}$  and VB ( $v_c = 150$  m/min) = 527  $\mu\text{m}$ ) after a cutting length of 4030 m. Here, the residual stress in the workpiece surface is increased to approx. 128 MPa and

257 MPa, respectively. The only cutting tool showing no flank wear land width was used in a cutting speed regime of 50 m/min. The highest built-up edge visible on the cutting tool leading to lowest wear (flank wear land width VB was measured to be 0  $\mu\text{m}$ , only radius wear and notch wear are increasing with cutting length). The cutting conditions of  $v_c = 50$  m/min resulted in a compressive residual stress state of about  $-60 \pm 25$  MPa that is constant to a depth of about 75  $\mu\text{m}$  for the smaller (1332 m) and higher cutting length (4030 m). The tensile residual stress gradients for the higher tool wear and cutting speeds are steeper, whereas the IB-profiles shown in Fig. 5 have a similar decaying trend as previously shown in Fig. 4 for the results after 4 machining passes. Only the IB depth profile for  $v_c = 50$  m/min has a steeper gradient as compared to the IB-profiles for the workpieces machined with 100 m/min – 150 m/min (see Fig. 5). This effect is attributed to lower cutting temperatures due to lower cutting speeds and tool wear.

The comparison of the residual stress depth profiles obtained, the profiles determined for workpieces machined with the highest built-up edge detected had the most uniform stress distribution (lowest stress gradient). In contrast to that the surface roughness is more inhomogeneous due to the breaking off of small particles from the built-up edge. In conclusion, the higher built-up edge height leads to a more homogeneous residual compressive stress depth profile. The higher cutting speeds lead to higher tool wear rates at the same time lower built-up edge tendencies. Only tensile residual stresses are measured for progressive tool wear. These higher tensile residual stresses are ascribed to tool wear induced higher cutting temperatures [3,7].

### Summary

In summary the effect of built-up edge effect on residual stress state in machined workpieces could be shown. Only small compressive stresses are introduced to a depth of 75  $\mu\text{m}$  for the cutting parameters leading to most pronounced built-up edges. Higher tensile stresses are determined for higher cutting speeds due to higher cutting temperatures. This tendency is more distinct for high tool wear, where tensile stresses are increased, which is also comparable to related literature [3].

### References

- [1] J. Kümmel, J. Gibmeier, E. Müller, R. Schneider, V. Schulze, and A. Wanner. Detailed analysis of microstructure of intentionally formed built-up edges for improving wear behaviour in dry metal cutting process of steel. *Wear*, 311(1-2):21-30, 2014.
- [2] B. Scholtes. Eigenspannungen in mechanisch randschichtverformten Werkstoffzuständen: Ursachen, Ermittlung und Bewertung, DGM-Informationsgesellschaft, Oberursel, 1991.
- [3] J. Paulo Davim. *Surface Integrity in Machining*. Springer London, London, 2010.
- [4] I.S. Jawahir, E. Brinksmeier, R. M'Saoubi, D.K. Aspinwall, J.C. Outeiro, D. Meyer, D. Umbrello, and A.D. Jayal. Surface integrity in material removal processes: Recent advances. *CIRP Annals - Manufacturing Technology*, 60(2):603-626, 2011.
- [5] H. Autenrieth. Numerische Analyse der Mikrozerspannung am Beispiel von normalisiertem C45E. Dissertation, Universität Karlsruhe, 2010.
- [6] C.R. Liu and M.M. Barash. Variables governing patterns of mechanical residual stress in a machined surface. *Journal of Engineering for Industry*, 104:257-264, 1982.
- [7] Q. Xie, A.E. Bayoumi, and L.A. Kendall. On tool wear and its effect on machined surface integrity. *Journal of Materials Shaping Technology*, 8:255-265, 1990.
- [8] E. Macherauch and P. Müller. Das  $\sin^2\psi$ -Verfahren in der röntgenographischen Spannungsmessung. *Zeitschrift für angewandte Physik*, 13:305–316, 1961.
- [9] B. Eigenmann and E. Macherauch. Röntgenographische Untersuchung von Spannungszuständen in Werkstoffen Teil III. *Materialwissenschaft und Werkstofftechnik*, 27(9):426–437, 1996.
- [10] U. Wolfstieg. Die Symmetrisierung unsymmetrischer Interferenzlinien mit Hilfe von Spezialblenden. *HTM - Härterei-Technische Mitteilungen*, 31:23–26, 1976.